

References and Notes

1. J. A. Eddy and A. A. Boornazian, *Am. Astron. Soc. Bull.* **11**, 437 (1979); see also *Phys. Today* **32** (No. 9), 17 (1979).
2. Seeing conditions, as well as activity near the solar limb, make very difficult the determination of the "proper" instants of contact, despite the pains taken to define these instants operationally as in the instructions distributed by the U.S. Naval Observatory to potential observers of the 1940 transit [G. M. Clemence and G. C. Whittaker, *U.S. Nav. Observatory Publ.* **15** (pt. 2), 25 (1942)]: "At the time of contact I Mercury begins to impinge on the Sun's disk. Its apparent diameter is nearly 10 seconds of arc, or about 1/200 that of the Sun. About a minute and a half later will occur a phenomenon which may be mistaken for contact II. At this instant Mercury appears to be internally tangent to the Sun's limb, but light is not yet visible all the way around the planet. This is *not* the time of contact II. About this time the black drop usually begins to form and ten seconds later Mercury will appear as a black drop hanging on the Sun's limb. Several seconds later the black drop will break away from the Sun's limb and this is the time of true contact II. At this instant a thread of light becomes visible between the planet and the Sun's limb. Although this phenomenon is perfectly well defined the time of its occurrence is often uncertain by more than ten seconds. The boiling of the Sun's limb, particularly when low in the sky, makes the observation difficult. Sometimes the thread of light appears to be made and broken several times in quick succession. In such cases the interval when it was being made and broken must be noted. In rare instances no black drop may be noticed. "Five hours later a similar sequence of events takes place in reverse order as Mercury passes off the Sun's disk. Here the phenomenon to be observed is the breaking of the thread of light between Mercury and the Sun's limb."
3. See, for example, U. J. J. Leverrier, *Ann. Obs. Paris* **5**, 1 (1859); S. Newcomb, *Astron. Pap. Am. Ephemeris* **1** (pt. 6), 363 (1882); R. T. A. Innes, *Circ. Union Obs. S. Afr.* **65**, 303 (1925); K. P. Williams, *Indiana Univ. Publ. Sci. Ser. No. 9 and Suppl.* (1939); G. M. Clemence, *Astron. Pap. Am. Ephemeris* **11** (pt. 1), 1 (1943); L. V. Morrison and C. G. Ward, *Mon. Not. R. Astron. Soc.* **173**, 183 (1975).
4. The mean times of the contacts, for each transit through 1940, reduced to equivalent geocentric values, were obtained from earlier publications (3). For the last five transits, 1953 through 1973, individual observations were gathered from published accounts and analyzed by M. Ash and me (unpublished). The mean times of the contacts were treated as independent, Gaussian random variables with the standard error in each case based on the distribution of the individual observations of the time of contact. However, in no case was the standard error taken to be less than 5 seconds.
5. As an external check on our differenced residuals, $\Delta t_3 - \Delta t_2$, I compared them to the values obtained by Newcomb, by Innes, and by Williams [neither Clemence nor Morrison and Ward (3) reported results in a form amenable for comparison, and the overlap with the values from Leverrier was too meager to be useful]; the unweighted means of the absolute values of the differences were 3.8, 3.6, and 5.5 seconds, respectively, for the data common to our analysis and each of theirs. The corresponding means for the pairwise differences between their residuals ranged from 4.7 to 6.1 seconds. (Before making these comparisons, I changed the residuals given by Innes to correct for the time variation of the diameter of the sun obtained in his solution; see below.) It is not clear why these differences are so large, but it is clear from point-by-point comparisons that such changes in the residuals would not alter my conclusions.
6. This value is smaller than the accepted value of the diameter of the sun by about 0.6 arc second [see, for example, C. W. Allen, *Astrophysical Quantities* (Athlone, London, 1963), p. 162]. The sign of this difference could be expected on the basis of the operational definition of a transit (2).
7. The residuals shown for the transits observed between 1700 and 1750 were obtained from Newcomb's analysis (3) and are therefore not strictly compatible with the remainder of the 23, which were based on our analysis of the optical, radar, and transit data. Observations made before 1700 were deemed useless (3); in addition, data from 13 transits after 1700 were omitted since, for these, at most one internal contact was observed reliably (3). The relatively large spread in the mid-20th-century values of ΔD_{\odot}

may be due to the far higher proportion of amateur observers for the recent than for the earlier transits and to the lack of application to the recent data (4) of the painstaking sorting procedure used to analyze the earlier observations. To give the flavor of the latter analysis, I quote two excerpts from Newcomb (3): "Looking at the general agreement among the observers of external contact, it can hardly be doubted that Mercury was entirely off the sun before $9^{\text{h}}0^{\text{m}}$. If this be so, there must have been an error of half a minute or more in the times of the observers at Haarlem and The Hague. One of these is entirely unnamed, the other was not an astronomer. Their results may, therefore, be rejected without question" (p. 390). "Williams used a watch without a second hand, which was set by transits. Except for the possibility of systematic errors in the other observations, his result should be rejected. In view of this possibility, we may assign it the weight 1/3" (p. 392). The need for such extraordinary observation-by-observation analysis was dictated by the presence of systematic errors that caused the tail of the distribution of timings for most contacts to be overpopulated (platykurtic) relative to expectations based on a normal distribution.

8. The standard errors are based on a uniform scaling of the errors shown in Fig. 2 by a factor of

0.8 such that the root weighted mean square of the postfit residuals is unity.

9. Innes (3) also estimated the centennial change in the diameter of the sun from the transit data obtained before 1925. He found a change of 0.56 ± 0.10 arc second per century, which he attributed to the effects of the use of more powerful optics for observations of the later transits. I cannot explain the difference between Innes's results and mine as I did not attempt to reproduce his calculations.
10. S. Sofia *et al.*, *Science* **204**, 1306 (1979).
11. Eddy's analysis (1) actually indicated a substantial difference in the rates of change of the equatorial and polar diameters of the sun, with the former being about -2 and the latter about -0.8 arc second per century. In view of my far smaller bound on any change in the diameter, it seemed pointless to investigate possible differences in the rates of change of the equatorial and polar diameters from the transit data.
12. I thank F. Amuchastegui, A. Forni, and especially M. E. Ash for their important aid in the original analysis of the transit data, and C. C. Counselman, III, for a critical reading of the manuscript. This work was supported in part by NSF grant PHY 78-07760.

16 November 1979

Magnetic Field of a Nerve Impulse: First Measurements

Abstract. *The magnetic field of the action potential from an isolated frog sciatic nerve was measured by a SQUID magnetometer with a novel room-temperature pickup coil. The 1.2×10^{-10} tesla field was measured 1.3 millimeters from the nerve with a signal-to-noise ratio of 40 to 1.*

Although the electrical potentials produced by a propagating nerve action potential can be measured readily, the accompanying magnetic fields have thus far never been observed directly. The failure of previous attempts is readily understood. The nerve action potential has the form of a moving, azimuthally symmetric solitary wave (I) which can be modeled as two opposing current dipoles driven by a potential change of the order of 70 mV. The peak currents range (2) from 5 to 10 μA . The external magnetic

field B can be estimated from Ampere's law, in which I is the net axial current enclosed by a closed path of integration c

$$\oint_c \mathbf{B} \cdot d\mathbf{l} = \mu_0 I \quad (1)$$

where μ_0 is the magnetic permeability of free space, and the dot (inner) product between \mathbf{B} and $d\mathbf{l}$, the differential element that describes c , is integrated over the complete length of the path.

If the nerve is immersed in a conducting medium, the maximum magnetic field of 10^{-10} T occurs at the nerve surface (radius $r \leq 0.3$ mm), with the numbers depending upon the preparation used. As the distance from the nerve is increased, an increasing fraction of the external current returns within c , so that the field at 1 cm is a few picoteslas and decreases thereafter in proportion to the inverse cube of the distance (3). The weakness of the magnetic field, its rapid falloff with distance, and the required 1- to 2-kHz bandwidth place the signal at the limit of detectability of magnetometers used for biomagnetic measurements (4).

Two groups of investigators have used large room-temperature coils and conventional amplifiers to obtain signals interpreted as the magnetic field from the action potential of an isolated frog sciatic nerve (5). These signals did not exhibit the expected reversal of polarity upon reversal of the direction of impulse propagation, and the measurements were

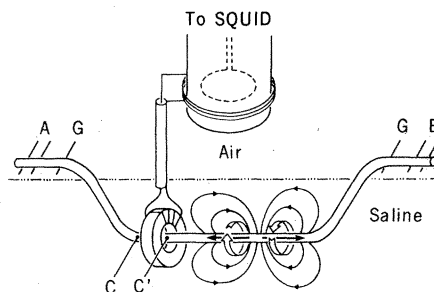
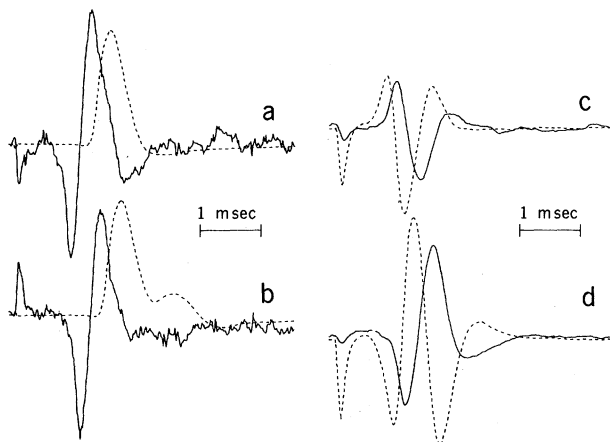


Fig. 1. Diagram of the experiment (not to scale). A nerve action potential propagates from proximal to distal (left to right in the figure). The wide and narrow arrows around the nerve represent the magnetic and electric field, respectively; the arrows on the nerve axis are equivalent dipole sources. Stimulation may be from either electrodes A or B, with the other or C as recording electrodes. The toroidal pickup coil is connected to a large transfer coil around the cylindrical Dewar vessel that contains the SQUID magnetometer and its pickup coil (indicated by dashed lines) surrounded by liquid helium.

Fig. 2. The magnetic field (solid lines) and electric potential (dashed lines) of an isolated frog sciatic nerve. The recordings in (a) and (b) were made with opposite polarities of the 1.6-V, 20- μ sec stimulus. As evidenced by the initial stimulus artifact, the stimulus was negative (cathode toward toroid) in (a) and positive in (b); in both cases it was applied to electrodes A (as in Fig. 1), with the electrical recordings made in air from B (as in Fig. 1) referenced to the grounded saline bath. The magnetic signal is the average of 256 traces recorded in a 1-Hz to 5-kHz bandwidth, with the first peak having an amplitude of 70 pT; the electric signal is the average of 128 traces in a 1-Hz to 1-kHz bandwidth. The late peak in (b) is due to slow beta fiber activity. The recordings in (c) and (d) were made with opposite directions of impulse propagation. In (c), the 0.5-V negative stimulus was applied at A (Fig. 1) and the electrical recording was made in the saline Ringer solution at C (Fig. 1); in (d) the stimulus was applied at B (Fig. 1) and the electrical recording again made at C (Fig. 1). The magnetic and electric signals are the average of 1024 and 128 traces, respectively, in a 0.01-Hz to 1-kHz bandwidth. The amplitude of the first magnetic peak is 60 pT.



made with a nerve supported in air so that all of the electrical currents were confined to the nerve bundle and the coaxial layer of moist electrolyte surrounding it (6). As a consequence, there could be no magnetic field in the air outside such a nerve. These previous measurements may have been sensitive to capacitive coupling, since three electrostatically shielded pickup coils of adequate sensitivity were unable to detect the magnetic field of a moist nerve in air (7). Our measurements avoid this difficulty in that we used a nerve immersed in a conducting medium.

Sciatic nerves from bullfrogs (*Rana catesbeiana*) were dissected and placed in a dish containing aerated Ringer solution. The nerve was gently laid over an arrangement of chlorided silver wire electrodes (Fig. 1) so it could be electrically stimulated proximally and the action potential could be recorded distally, or vice versa. The magnetic fields were recorded with a SQUID (superconducting quantum interference device) magnetometer (8) [1.3×10^{-14} T (Hz) $^{-1/2}$ sensitivity (9), 18.7 mV per flux quantum calibration]. The SQUID magnetometer detects magnetic flux changes through a superconducting pickup coil in a liquid helium environment. At the closest coil-to-nerve separation of 15 mm, the nerve magnetic field could barely be detected.

Considerable effort was thereby expended to increase the signal-to-noise ratio. The distance between the nerve and the detector coil was reduced an order of magnitude by threading the nerve through a specially constructed miniature toroidal transformer (10). The

transformer consisted of four turns of wire (No. 38) wound on a 1.2-mm-thick ferrite core (minor diameter, 1.2 mm; major diameter, 2.6 mm; and effective relative permeability of 6800 at 2000 Hz). The effective cross-sectional area of this toroidal pickup coil was 3.9×10^{-2} m 2 . The toroid was inductively coupled (mutual inductance, 5.4 nH) to the magnetometer face coil by a transfer coil wrapped around the outside of the Dewar. Experiments were performed in an area isolated from large magnetic objects and magnetic transients. The 60-Hz noise was further reduced by analog cancellation. By averaging 1024 or more repetitive signals (0.5- to 1.5-mV signal, 0.4-mV random SQUID noise, 1.5-mV power line harmonics) with a Nicolet 1170 signal averager, signal-to-noise ratios of 30 to 40 were obtained with a 1-kHz bandwidth.

Figure 2 shows the magnetic (solid lines) and electric (dashed lines) signals recorded from a frog sciatic nerve immersed in Ringer solution. The proximal end of the nerve was stimulated by means of the A electrodes (Fig. 1) 23 mm from the toroid. The action potential was recorded in air 15 mm distal to the toroidal coil by a single B electrode referenced to the grounded saline bath. The stimulus was negative (cathode nearest toroid) (Fig. 2a) and positive (Fig. 2b). The magnetic field of the stimulus current, visible at the beginning of the traces, reverses polarity when the stimulus is reversed. As expected, the magnetic and electric signals of the action potential do not reverse.

The electric trace in Fig. 2a exhib-

its a small stimulus artifact and has the shape of action potentials reported previously (11), with a rather steep initial portion followed by a slower region of recovery; the average asymmetry in our work was 1.9 to 1. The differing delays between the stimulus and the onset of the electric and magnetic signals are due to the separation of the toroid and the B electrodes and to the measured (22 m/sec) conduction velocity. In the electric signal shown in Fig. 2b, the positive stimulus activated a slower set of beta nerve fibers (12), and a corresponding shoulder is visible on the magnetic record.

The magnetic signal is produced predominantly (see below) by the total axial current I_z enclosed by the toroid while the voltage action potential in air expresses the charge on the membrane. The magnetic trace should then be proportional to the first derivative of the electric trace, as observed in Fig. 2. On exchange of the stimulating and recording electrodes, the magnetic signal must reverse sign (Fig. 1) since the leading current loop reverses direction; but the single-ended voltage trace should be similar. When this experiment was performed, the magnetic signals reversed as expected and had a common mode portion of only one part in seven while the electric signals did not reverse, verifying that the magnetometer signal represents the magnetic field of the action potential and not capacitive coupling to the electric field.

Since more detailed interpretation of the data in Fig. 2, a and b, is hindered by the separation between the toroid and the recording electrodes, the recordings in Fig. 2, c and d, were obtained with a pair of spherical electrodes (C and C' in Fig. 1) with a 5.3-mm separation placed in close proximity to the nerve as it passed through the toroid. This arrangement provided coincident magnetic and electric data but the electric measurement had to be made in the saline bath. We show records for distal and proximal stimulation in Fig. 2, c and d, respectively; the reversal of the magnetic trace (solid line) is apparent, and the crossover of the magnetic trace occurs at the peak in the electric signal. Since the electric trace is differential, it measures $dV(z)/dz$, which is proportional to the axial return current, in the saline adjacent to the nerve. It must therefore reverse when the direction of impulse propagation reverses, in contrast to the potential recorded by single-ended measurements in air. Also, we would expect (3, 13) precisely the derivative relationship between the electric and magnetic

traces in Fig. 2, c and d. Thus the first peak of the magnetic trace indicates the forward loop of the currents in the moving action potential. By Ampere's law, the toroidal coil measures that part of the axial nerve current which is not canceled by return flow within the toroid. The current paths must be known in detail to determine precisely what fraction of the total nerve current is measured.

Further checks of the magnetic signals were performed. When the coils were tied to ground, rather than left floating electrically, much larger electrical artifacts were produced. Removal of the saline, so that only a slight amount of current could circulate around the still moist surface of the toroid, resulted in large, immediate signal reductions. Also, an artificial electric current dipole was made by applying a square voltage pulse to a twisted pair of No. 34 wires with bared, separated ends immersed in the saline. When this source threaded the toroid, a large signal was received; when it was oriented so that substantial field cancellation was expected, the signal dropped by a factor of 5 although the saline surrounding the toroid underwent an identical voltage excursion.

The toroid sensitivity was calculated and measured as a function of frequency (f) ($80 \text{ Hz} < f < 10 \text{ kHz}$). Since the coil has resistance R in addition to inductance L , the true magnetic field waveform $B(t)$ has an additional small component proportional to the integral of the observed signal $B'(t)$ multiplied by R/L for the toroid (10). Thus

$$B(t) = B'(t) + R/L \int B'(t') dt' \quad (2)$$

with a calibration of 150 pT/mV. While the exact calculation of this correction requires inclusion of the effect of the low-pass filter (10), the R/L effect is small during the early part of the action potential. To show this, we approximate the first magnetic peak in Fig. 2d by a Lorentzian profile of height $h = 4.8 \text{ mV}$ and width $w = 89 \mu\text{sec}$. Then Eq. 2 becomes

$$B(0) = B'(0) + 0.30 h/w \tan^{-1}(500/89) \quad (3)$$

resulting in a field of 125 pT at the first peak ($t = 0$) of which 27 percent is due to the second, correction term. This represents a net current through the toroid of $0.8 \pm 0.2 \mu\text{A}$ in the forward loop of the action potential, with a precision adequate for the exploratory purposes of this work. Larger currents and larger fields will, of course, exist closer to the nerve fibers.

Even at their semiquantitative level, these experiments demonstrate that

magnetic measurements of nerve function can be made directly in the conducting fluid; unlike electrical signals, they are not obliterated by the high conductivity fluid. The use of a split toroid will allow measurements on living systems without requiring puncture or intrusive contact with the nerve axon. More important, this technique measures current density directly (14) and allows determination of current profiles without assumptions about conductivity and electric boundary conditions that are necessary to unfold the nerve current from voltage recordings (15). Since the magnetic trace is very close to an actual current measurement, it is therefore a particularly strong complement to the electrical record.

JOHN P. WIKSWO, JR.

JOHN P. BARACH

Department of Physics and Astronomy,
Vanderbilt University,
Nashville, Tennessee 37235

JOHN A. FREEMAN

Department of Anatomy,
Vanderbilt University School of
Medicine, Nashville 37232

References and Notes

1. A. C. Scott, *Rev. Mod. Phys.* **47**, 487 (1975).
2. B. Katz, *Nerve, Muscle and Synapse* (McGraw-Hill, New York, 1966).
3. K. R. Swinney and J. P. Wiksw, Jr., *Biophys. J.*, in press.
4. M. Reite and J. Zimmerman, *Annu. Rev. Biophys. Bioeng.* **7**, 167 (1978).
5. J. H. Seipel and R. D. Morrow, *J. Wash. Acad. Sci.* **50** (No. 6), 1 (1960); J. A. Gengerelli, N. J. Holter, W. R. Glasscock, *J. Psychol.* **57**, 201 (1964); *ibid.* **52**, 317 (1961).
6. A. Kolin, *Phys. Today* **21** (No. 5), 39 (1968).
7. A. M. Cook and F. M. Long, in *The Nervous System and Electric Currents*, N. L. Wulfsohn and A. Sances, Eds. (Plenum, New York, 1970), pp. 9-13.
8. SHE model BMP-55; S.H.E. Corp., 4174 Sorrento Valley Blvd., San Diego, Calif. 92121.
9. J. P. Wiksw, Jr., *AIP Conf. Proc.* **44**, 145 (1978).
10. J. P. Barach *et al.*, in preparation.
11. R. Lorente de N6, *Studies Rockefeller Inst. Med. Res.* **132**, 384 (1947).
12. J. Erlanger and H. S. Glasser, *Electrical Signs of Nervous Activity* (Univ. of Pennsylvania Press, Philadelphia, 1937).
13. J. Clark and R. Plonsey, *Biophys. J.* **8**, 842 (1968).
14. Properly it measures curl J , but in simple axon geometries, Stokes' theorem is used at once (3).
15. R. K. Hobbie, *Intermediate Physics for Medicine and Biology* (Wiley, New York, 1978), pp. 178-203.
16. We thank J. K. Wiksw, J. Madey, E. Iufer, R. Debs, and J. Barnes for their encouragement and H. Sadisky for the ferrite cores. Supported in part by grants from the Research Corporation and the Vanderbilt University Research Council, and by NIH biomedical research support grant RR07089-13.

24 September 1979; 6 December 1979

Localization of Lysyl Oxidase in Hen Oviduct: Implications in Egg Shell Membrane Formation and Composition

Abstract. *Lysyl oxidase activity was found in the isthmus (the membrane-forming region) of the hen's oviduct in a copper-rich region proximal to the shell gland. Desmosine and isodesmosine, cross-linking compounds associated with mature elastin, were found in hydrolysates of the shell membrane, confirming the necessity for lysyl oxidase in its biosynthesis. Shell membranes from hens fed a copper-deficient diet or a diet supplemented with β -aminopropionitrile had a reduced content of desmosine and isodesmosine.*

Although early studies classified the protein in egg shell membranes as keratin (1), recent investigations established that the membrane is composed in part of proteins resembling those in connective tissue. Upon acid hydrolysis, the material yields hydroxylysines (2), hydroxyprolines (3), and desmosines (4), suggesting the presence of protein components bearing a structural resemblance to collagen and elastin (5). Moreover, shell formation is frequently defective in hens fed diets deficient in copper (6) or supplemented with the lathrogen β -aminopropionitrile (BAPN) (7); both treatments affect connective tissue protein metabolism by preventing the formation of cross-links. The molecular target is lysyl oxidase, which catalyzes a specific oxidative deamination of lysines that is obligatory to formation of the cross-links. The requirement of copper (8, 9) and the inhibition of the enzyme by

BAPN (10) are well established. A recent study (6) showed that lysine residues in shell membrane proteins are oxidized less in copper-deficient hens than in copper-supplemented hens. The data suggest that the shell membrane is formed through a process not unlike that which forms other connective tissue proteins. Thus we hypothesize that lysyl oxidase is required in the biogenesis of shell membrane protein. Evidence is presented here to support this hypothesis.

Oviduct tissue was obtained from sexually mature hens at the onset of the laying period. Segments (2.54 cm) from the entire length of the tube were examined for enzyme activity. The segments were weighed, minced, and homogenized in buffer (0.12M NaCl and 0.015M potassium phosphate, pH 7.6). The tissue was isolated by centrifugation, resuspended in a urea buffer (4M urea in 0.01M NaCl and 0.002M potassium phosphate, pH